ELSEVIER

Chemical Physics 238 (1998) 401–406

Chemical Physics

Charge transfer between Si^{3+} and helium at thermal and low energies

P. Honvault [a,b], M.C. Bacchus-Montabonel [b], M. Gargaud [c], R. McCarroll [a]

[a] *Laboratoire de Dynamique Moléculaire et Atomique (URA 774 du CNRS), Université Pierre et Marie Curie, 4 Place Jussieu, 75252 Paris Cedex 05, France*

[b] *Laboratoire de Spectrométrie Ionique et Moléculaire (UMR 5579 du CNRS), Université Lyon I, 43, Bd du 11 Novembre 1918, 69622 Villeurbanne Cedex, France*

[c] *Observatoire de l'Université de Bordeaux I (INSU / CNRS URA 352), B.P. 89, 33270 Floirac, France*

Received 8 July 1998

Abstract

Cross sections and rate coefficients for selective electron capture and excitation in Si^{3+}–He collisions in the thermal-eV energy range are calculated using a quantum mechanical method. It is confirmed that electron capture to the ground state of Si^{2+} is the dominant charge transfer mechanism and that the inverse process in which He^+ captures an electron in a collision with ground state Si^{2+} can occur easily. © 1998 Elsevier Science B.V. All rights reserved.

1. Introduction

A quantitative analysis of the emission-line spectra of ionized astronomical objects (such as planetary nebulae, nova shells, active galactic nuclei, etc.) requires reliable data on the microscopic ionization and recombination processes involved. Recombination may occur either by radiative (or dielectronic) capture or by charge transfer from neutral species. The charge transfer recombination process with atomic hydrogen or helium is particularly important in astrophysical plasmas for many doubly or triply charged ions, whose emission lines are used to furnish direct information on the ionization structure of astronomical objects. Emission and absorption lines of Si^+, Si^{2+}, and Si^{3+} are observed in many spectra [1–5]. The intensity line ratios of Si^{2+} are used to deduce electron temperature and density in emissive regions [6–8].

As a general rule, charge transfer recombination of an ion with charge q leads to the formation of an excited state with charge $q-1$. In a dilute medium (such as the astronomical emission-line objects), these states decay radiatively to the ground state before a collision occurs. In that case, the inverse charge transfer ionization is ineffective. On the other hand, there are some doubly and triply charged ions for which electron capture can lead directly to the formation of ground states. When this occurs, ionization may also occur rapidly via the inverse charge transfer process.

Two important reactions of this kind are the following

$$Si^{2+}(3s^2)^1S + H(1s)^2S \leftrightarrow Si^+(3s^2 3p)^2P + H^+ \quad (1)$$

$$Si^{3+}(3s)^2S + He(1s^2)^1S \leftrightarrow Si^{2+}(3s^2)^1S + He^+(1s)^2S \quad (2)$$

0301-0104/98/$ - see front matter
PII: S0301-0104(98)00331-0

These reactions are critical in determining the fractional abundances of the Si^{q+} ions for $q = 1, \ldots, 4$. Baliunas and Butler [9] show that inclusion of these two charge transfer reactions change significantly the Si^{2+} and Si^{3+} abundance ratios in coronal-type plasmas for temperatures in the range $10^4 < T < 10^5$ K. Because of the inverse reaction (2), the Si^{3+} abundance is increased and is dominant over a wide temperature range.

Reaction (1) has been investigated theoretically [10,11] using model potential methods to represent the Si^{2+} core electrons. As for reaction (2), there have only been empirical estimates [12] of the cross section. In this work we shall not consider the Si^{3+}/H charge transfer reaction, since it takes place via capture to an excited state of Si^{2+}. For that reason charge transfer ionization of Si^{2+} by H^+ is ineffective.

The Si^{3+}/He reaction (2) is also of interest as a bench-mark for low energy experiments. At present, there are serious disagreements between some of the new ion-trap measurements [13] and theoretical predictions [14], which are difficult to understand. For example, no reasonable conjecture seems able to explain why the measured reaction rate for O^{2+}/He charge exchange at thermal energies is a factor of 1000 smaller than the theoretical results [14,15]. The Si^{3+}/He system would appear to be a better candidate for comparing experiment [13] and theory. As in the case for the O^{2+}/He system, theory predicts a large cross section at thermal energies, but the Si^{3+}/He system is less likely to be affected by contamination from metastable states.

2. Theory

The methods used in this work are similar to those used for recent work on the O^{2+}/H and O^{2+}/He systems [14,16,17]. Only the basic essentials of the theoretical model are recalled here.

Although we shall mainly be concerned with reaction (2), we consider the complete network of asymptotic channels interacting with both ground $(3s)^2S$ and excited $(3p)^2P$ states of Si^{3+} ions. The reason is that while at astrophysical energies (0.1–10 eV) there is little interference from adiabatic states to the $(3p)^2P$ state of Si^{3+}, such is not the case at higher energies where coupling to the $(3p)^2P$ channels can become appreciable. We shall assume spin-orbit coupling to be of negligible importance in the electron capture process so that electron spin is conserved in the collision process. We need therefore consider only the network of doublet states correlated to the entry channel. The possible reaction channels (and the asymptotic states to which they are correlated) are designated as follows:

$$Si^{2+}(3s^2)^1S + He^+(1s)^2S \quad {}^2\Sigma^+ \tag{3}$$

$$Si^{2+}(3s3p)^3P + He^+(1s)^2S \quad {}^2\Sigma^+ \tag{4}$$

$$Si^{3+}(3s)^2S + He(1s^2)^1S \quad {}^2\Sigma^+ \tag{5}$$

$$Si^{2+}(3s3p)^1P + He^+(1s)^2S \quad {}^2\Sigma^+ \tag{6}$$

$$Si^{3+}(3p)^2P + He(1s^2)^1S \quad {}^2\Sigma^+ \tag{7}$$

$$Si^{2+}(3s3p)^3P + He^+(1s)^2S \quad {}^2\Pi^{\pm} \tag{8}$$

$$Si^{2+}(3s3p)^1P + He^+(1s)^2S \quad {}^2\Pi^{\pm} \tag{9}$$

$$Si^{3+}(3p)^2P + He(1s^2)^1S \quad {}^2\Pi^{\pm} \tag{10}$$

$$Si^{2+}(3p^2)^1D + He^+(1s)^2S \quad {}^2\Sigma^+, {}^2\Pi, {}^2\Delta \tag{11}$$

$$Si^{2+}(3s3d)^1D + He^+(1s)^2S \quad {}^2\Sigma^+, {}^2\Pi, {}^2\Delta \tag{12}$$

$$Si^{2+}(3p^2)^3P + He^+(1s)^2S \quad {}^2\Sigma^-, {}^2\Pi \tag{13}$$

The potential energy curves of the manifold of the $^2\Sigma^+$ and $^2\Pi$ states, correlated to channels 3–13 have been calculated for interatomic distances in the 2–25 a_0 range by an *ab-initio* configuration interaction method based on the CIPSI algorithm [18,19]. A non-local pseudo-potential [20] has been used to represent the core electrons of the Si atom. The calculations have been performed with CI spaces of about 300–400 determinants for the zeroth-order diagonalization with a threshold $\eta = 0.01$ for the contribution to the perturbation.

The basis of atomic functions is presented in Table 1. For Si, we have constructed a 9s7p2d basis of Gaussian functions, contracted to 5s4p2d, starting from the basis sets of McLean and Chandler [21]. The exponents and contraction coefficients have been optimized on the $Si^{3+}(3s)^2S$ and $Si^{2+}(3s3p)^3P$. For He, we have chosen the 4s1p basis already used in previous applications [22]. A reasonably good agreement with the experimental values of Bashkin and Stoner [23] is observed for a large number of Si^{2+}

Table 1
Exponents and contraction coefficients of the Gaussian basis set of Si and He

	S		P		D	
	Exp.	Cont. coeff.	Exp.	Cont. coeff.	Exp.	Cont. coeff.
Si	657.47	−0.000024	95.352	−0.000175	0.5	1.0
	214.00	0.000016	30.334	−0.000102	0.2	1.0
	77.606	−0.000377	10.944	−0.004648		
	30.640	0.000229				
	12.816	−0.002738	4.042	0.011817		
			1.908	−0.037812		
	3.027	1.0				
	1.609	1.0	0.347	1.0		
	0.274	1.0	0.139	1.0		
	0.128	1.0				
He	97.709	0.00759	0.27	1.0		
	14.857	0.05413				
	3.373	0.21595				
	0.897	1.0				
	0.251	1.0				
	0.074	1.0				

and Si^{3+} energy levels (Table 2). This accuracy, which is better than 1% for the molecular energies in the dissociation limit, should be sufficient for a satisfactory description of the electron capture dynamics.

The radial coupling matrix elements between all pairs of states of the same symmetry have been calculated by means of the finite difference technique:

$$g_{KL}(R) = \langle \Psi_K | \partial / \partial R | \Psi_L \rangle = \lim_{\Delta \to 0} 1/\Delta \langle \Psi_K(R) | \Psi_L(R+\Delta) \rangle$$

with the parameter $\Delta = 0.0012$ au as previously tested and using the silicon nucleus as origin of electronic coordinates. The rotational coupling matrix elements $\langle \Psi_K | iL_y | \Psi_L \rangle$ between $^2\Sigma^+ - ^2\Pi$ and $^2\Pi - ^2\Delta$ molecular states have been determined directly from the quadrupole moment tensor [24].

Table 2
Atomic levels (eV): comparison with Bashkin and Stoner experimental levels

Levels	Calculation	Experiment
$Si^{3+}(3p)^2P$	41.972	42.367
$Si^{3+}(3s)^2S$	33.191	33.491
$Si^{2+}(3p^2)^3P$	15.896	16.113
$Si^{2+}(3s3d)^1D$	15.066	15.152
$Si^{2+}(3p^2)^1D$	15.072	15.152
$Si^{2+}(3s3p)^1P$	10.440	10.276
$Si^{2+}(3s3p)^3P$	6.392	6.568
$Si^{2+}(3s^2)^1S$	0.0	0.0

The potential energy curves are presented in Fig. 1. The potential energy curves of the $^2\Sigma^-$ and $^2\Delta$ states are not shown because they are weakly coupled to the main channels of interest (channels 3–10) which involve only states of $^2\Sigma^+$ or $^2\Pi$ symmetry. From a dynamical point of view, the ground state entry channel $[Si^{3+}(3s)^2S + He(1s^2)^1S]$ leads to a simple electron capture process. The potential energy curves exhibit a pronounced avoided crossing with $[Si^{2+}(3s^2)^1S + He^+(1s)^2S]$ around $R_X = 6.0\ a_0$. The crossing with channel $[Si^{2+}(3s3p)^3P + He^+(1s)^2S]$ around $R_X = 19.5\ a_0$ is strongly diabatic. At shorter internuclear distance, we notice an additional pseudo-crossing ($R_X = 3.2\ a_0$) between channels 4 and 5.

Although perhaps of academic interest, we may note that excited $Si^{3+}(3p)^2P$ ions will react both via $^2\Sigma^+$ and $^2\Pi$ channels to yield $[Si^{2+}(3s3p)^3P + He^+(1s)^2S]$ and $[Si^{2+}(3s3p)^1P + He^+(1s)^2S]$ channels. The potential energy curves show indeed two avoided crossings around $R = 7.0$ and $4.9\ a_0$ for the $^2\Sigma$ states and around $R = 7.25$ and $5.0\ a_0$ for the $^2\Pi$ states.

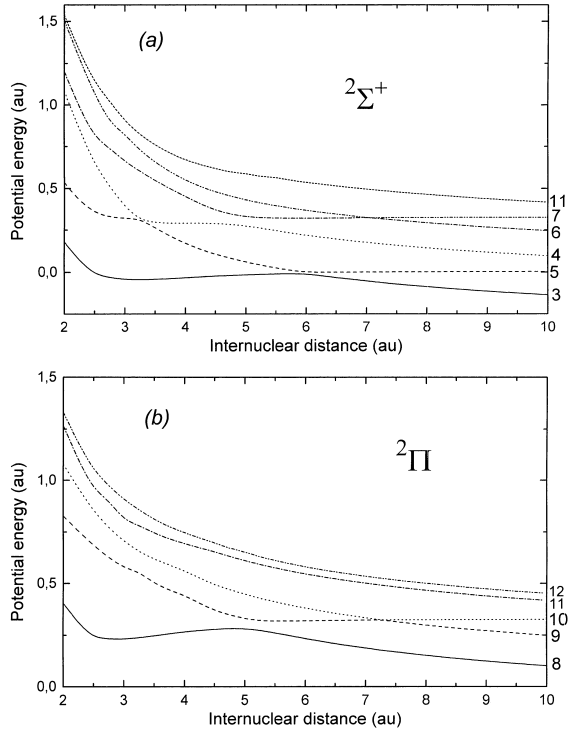

Fig. 1. Adiabatic potential energy curves for the $^2\Sigma^+$ (a) and $^2\Pi$ (b) states of $SiHe^{3+}$. The different channels are labeled as in the main text.

We report in Figs. 2 and 3 the corresponding radial and rotational matrix elements. The shape of these matrix elements is quite consistent with the results of Fig. 1. In particular the radial components reproduce quite well the $0.25\,a_0$ internuclear distance shift between the $^2\Sigma^+$ and $^2\Pi$ pseudo-crossing positions. The rotational coupling between the $[Si^{3+}(3p)^2P + He(1s^2)^1S]$ and $[Si^{2+}(3s^2)^1S + He^+(1s)^2S]$ channels is not shown.

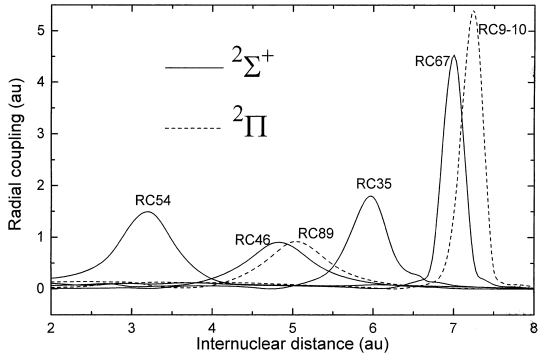

Fig. 2. Radial coupling (RC) matrix elements between $^2\Sigma^+$ (solid curves) and $^2\Pi$ (dashed curves) states of $SiHe^{3+}$. Same notations as in Fig. 1.

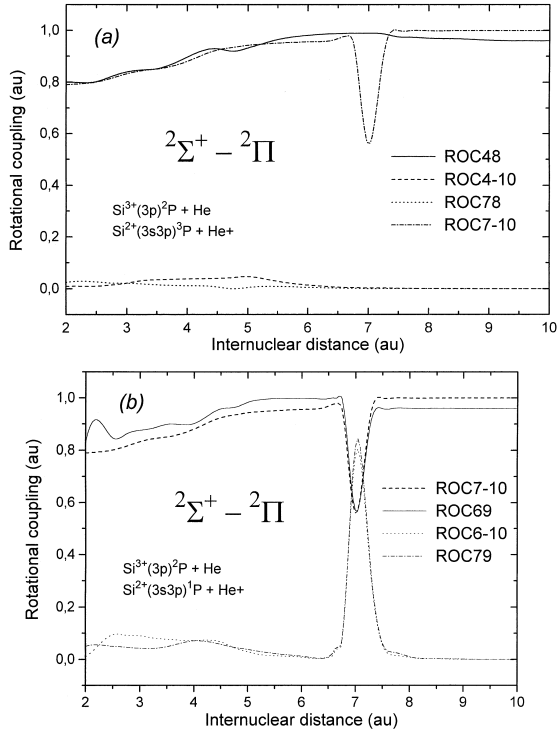

Fig. 3. Rotational coupling (ROC) matrix elements between $^2\Sigma^+$ (the first number) and $^2\Pi$ (the second number) states of $SiHe^{3+}$. The numerical notation is that used in Fig. 1. (a) With asymptotic notation, for $Si^{3+}(3p)^2P + He$ and $Si^{2+}(3s3p)^3P + He^+$. (b) With asymptotic notation, for $Si^{3+}(3p)^2P + He$ and $Si^{2+}(3s3p)^1P + He^+$.

The following seven reactions have been investigated simultaneously (channels 11, 12, 13 being decoupled from the entry channels).

$$Si^{3+}(3s)^2S + He(1s^2)^1S\,(\text{channel } 5)$$

$$\rightarrow Si^{2+}(3s^2)^1S + He^+(1s)^2S\,(\text{channel } 3) \quad (14)$$

$$\rightarrow Si^{2+}(3s3p)^3P + He^+(1s)^2S\,(\text{channels } 4,8) \quad (15)$$

$$\rightarrow Si^{2+}(3s3p)^1P + He^+(1s)^2S\,(\text{channels } 6,9) \quad (16)$$

$$\rightarrow Si^{3+}(3p)^2P + He(1s^2)^1S\,(\text{channels } 7,10) \quad (17)$$

$$Si^{3+}(3p)^2P + He(1s^2)^1S\,(\text{channels } 7,10)$$
$$\rightarrow Si^{2+}(3s^2)^1S + He^+(1s)^2S\,(\text{channel } 3) \quad (18)$$
$$\rightarrow Si^{2+}(3s3p)^3P + He^+(1s)^2S\,(\text{channels } 4,8) \quad (19)$$
$$\rightarrow Si^{2+}(3s3p)^1P + He^+(1s)^2S\,(\text{channels } 6,9) \quad (20)$$

plus the inverse charge transfer reaction:

$$Si^{2+}(3s^2)^1S + He^+(1s)^2S\,(\text{channel } 3)$$
$$\rightarrow Si^{3+}(3s)^2S + He(1s^2)^1S\,(\text{channel } 5) \quad (21)$$

At low energies, especially at thermal energies, the semi-classical formalism is difficult to apply since trajectory effects need to be accounted for. The collision dynamics have been treated by a quantum mechanical approach using the techniques developed for other applications [25]. Allowance for translation effects have been made by introduction of appropriate reaction coordinates [26,27]. This leads to a modification of the radial and rotational matrix elements similar in form to those resulting from the application of the Common Translation Factor (CTF) [28]. Subsequently a diabatic transformation of the basis set is first carried out before solving the coupled differential equations for the determination of the S matrix.

Table 3
Electron capture and excitation cross-sections (10^{-16} cm^2) as a function of incident ion energy in eV (laboratory system)

E (eV)	σ_1	σ_2	σ_3	σ_4	σ_{CT}
1.09	3.63				3.63
1.63	3.51				3.51
2.18	3.83				3.83
4.35	4.98				4.98
6.53	6.03				6.03
10.88	7.76				7.76
16.33	9.45				9.45
35.00	12.41				12.41
70.01	14.39				14.39
121.99	15.38	0.36	0.0001	0.0008	15.74
280.02	14.81	0.65	0.0003	0.03	15.46
630.07	13.47	0.69	0.0008	0.10	14.16
1120.1	12.14	0.64	0.0013	0.16	12.78
1750.5	11.13	0.60	0.0016	0.20	11.73
3499.3	9.87	0.49	0.0023	0.27	10.36
5262.4	9.07	0.41	0.0040	0.32	9.48
7000.7	8.84	0.37	0.0074	0.34	9.22

Table 4
Rate coefficients (10^{-9} cm^{3}s^{-1}) for charge transfer recombination (k_{CT}, k_{CT}^{Butler}) and ionization (k_{ion}, k_{ion}^{Butler})

T (K)	k_{CT}	k_{CT}^{Butler}	k_{ion}	k_{ion}^{Butler}
500	0.08		–	
1000	0.10	0.17	–	
2000	0.15		–	
3000	0.21	0.39	–	
5000	0.33		–	
10000	0.62	0.96	0.00002	0.00003
20000	1.14		0.0065	
30000	1.58	2.00	0.05	0.07
40000	1.97		0.15	
50000	2.31		0.29	
100000	3.60		1.28	1.21

3. Results

3.1. Cross sections

We report in Table 3 the charge transfer cross section results obtained for each reaction channel. Taking account of the statistical factors we obtained the following scheme for transitions originating from the ground state Si^{3+} ions:

$$\sigma_1 = \sigma_{5\rightarrow 3}$$
$$\sigma_2 = \sigma_{5\rightarrow 4} + \sigma_{5\rightarrow 8}$$
$$\sigma_3 = \sigma_{5\rightarrow 6} + \sigma_{5\rightarrow 9}$$
$$\sigma_4 = \sigma_{5\rightarrow 7} + \sigma_{5\rightarrow 10}$$

We define a total charge transfer cross section from ground state Si^{3+} ions: $\sigma_{CT} = \sigma_1 + \sigma_2 + \sigma_3$. Our calculations show (as expected) that capture to the ground state of Si^{2+} (reaction 14) is dominant, although there is a small contribution for energies higher than 120 eV from reaction (15) due to the inner crossing at $R_X = 3.2\ a_0$. The contribution of reaction (16) is always negligible whatever the energy involved. The cross section (σ_4) for excitation

of the Si^{3+} into the $(3p)^2P$ state becomes appreciable for energies above 600 eV.

3.2. Rate coefficients

For typical astrophysical temperatures only the ground state of Si^{3+} is significantly populated. The rate constant k_{CT} for charge transfer can then be easily obtained from the cross sections of Table 3 by averaging over a Maxwellian distribution of the kinetic energies of the collision partners. The results are presented in Table 4. The rate constant k_{CT} exceeds 10^{-9} cm^3s^{-1} over a wide temperature range (2×10^4 to 10^5 K). As T varies from 500 K to 10^5 K, k_{CT} increases from 0.08×10^{-9} cm^3s^{-1} to 3.52×10^{-9} cm^3s^{-1}.

Table 4 presents also rate coefficients obtained by Butler and Dalgarno [12]. They take into account only reaction (14). Their results are somewhat higher than ours, but bearing in mind the empirical nature of their theoretical model, the agreement is quite reasonable, nevertheless both theoretical approaches lead to cross sections lower than the ion-trap experimental point [13].

The rate constant k_{ion} for the reaction (21) can be obtained very simply from k_{CT} by the relations of micro-reversibility:

$$k_{ion} = g\exp\left(-\frac{\Delta E}{kT}\right)k_{CT}\,, \qquad (22)$$

where $g=1$ is the ratio of the statistical weights of the initial and final states and $\Delta E = 8.88$ eV is the energy gain of reaction (14). The rate constant k_{ion} is large for temperatures above 3×10^4 K. Below, it becomes rapidly negligible because of the exponential factor in (22).

4. Conclusion

The Si^{3+}–He system presents several unique features which make it an interesting candidate for experimental investigation in the low energy regime. The charge transfer mechanism is controlled by a single avoided crossing and there is little risk of interference with metastable states. The cross section is fairly large and exhibits an appreciable energy dependence in the eV range. All these factors should help in assessing the accuracy of *ab-initio* calculations of the molecular parameters (adiabatic energies and non-adiabatic couplings).

References

[1] M.A. Hayes, H. Nussbaumer, Astrophys. J. 161 (1986) 287.
[2] G.A. Doschek, L. Feldman, J.T. Mariska, J.L. Linsky, Astrophys. J. Lett. 226 (1978) L35.
[3] P.G. Judge, Mon. Not. Roy. Astr. Soc. 223 (1986) 239.
[4] W.A. Feibelman, Astrophys. J. 258 (1982) 548.
[5] G.D. Sandlin, J.D.F. Bartoe, G.F. Baureckner, R. Tousey, M.E. Van Hoosier, Astrophys. J. Suppl. 61 (1986) 801.
[6] P.L. Dufton, F.P. Keenan, A.E. Kingston, Mon. Not. Roy. Astr. Soc. 209 (1984) 1.
[7] H. Nussbaumer, Astron. Astrophys. 155 (1986) 205.
[8] F.P. Keenan, P.L. Dufton, A.E. Kingston, Mon. Not. Roy. Astr. Soc. 225 (1987) 859.
[9] S.L. Baliunas, S.E. Butler, Astrophys. J. 235 (1980) L45.
[10] R. McCarroll, P. Valiron, Astron. Astrophys. 53 (1976) 83.
[11] M. Gargaud, R. McCarroll, P. Valiron, Astron. Astrophys. 106 (1982) 197.
[12] S.E. Butler, A. Dalgarno, Astrophys. J. 241 (1980) 838.
[13] Z. Fang, V.H.S. Kwong, Astrophys. J. 483 (1997) 527. V.H.S. Kwong, Z. Fang, Phys. Rev. Lett. 71 (1993) 4127.
[14] M. Gargaud, M.C. Bacchus-Montabonel, R. McCarroll, J. Chem. Phys. 99 (1993) 4495.
[15] S.E. Butler, T.G. Heil, A. Dalgarno, J. Chem. Phys. 80 (1984) 4986.
[16] P. Honvault, M.C. Bacchus-Montabonel, R. McCarroll, J. Phys. B: At. Mol. Opt. Phys. 27 (1994) 3115.
[17] P. Honvault, M. Gargaud, M.C. Bacchus-Montabonel, R. McCarroll, Astron. Astrophys. 302 (1995) 931.
[18] B. Huron, J.P. Malrieu, P. Rancurel, J. Chem. Phys. 58 (1973) 5745.
[19] S. Evangelisti, J.P. Daudey, J.P. Malrieu, J. Chem. Phys. 75 (1983) 91.
[20] M. Pelissier, N. Komiha, J.P. Daudey, J. Comput. Chem. 9 (1988) 298.
[21] A.D. McLean, G.S. Chandler, J. Chem. Phys. 72 (1980) 5639.
[22] M.C. Bacchus-Montabonel, Phys. Rev. A 46 (1992) 217.
[23] S. Bashkin, J.O. Stoner, Atomic Energy Levels and Gotrian Diagrams, North Holland, Amsterdam, 1975.
[24] F. Fraija, A.R. Allouche, M.C. Bacchus-Montabonel, Phys. Rev. A 49 (1994) 272.
[25] M. Gargaud, J. Hanssen, R. McCarroll, P. Valiron, J. Phys. B: At. Mol. Opt. Phys. 14 (1981) 2259.
[26] M. Gargaud, R. McCarroll, P. Valiron, J. Phys. B: At. Mol. Opt. Phys. 20 (1987) 1555.
[27] R. McCarroll, D.S.F. Crothers, Advances in Atomic, Molecular and Optical Physics, vol. 32, D.R. Bates, B. Bederson (Eds.), Academic Press, New York, 1994, p. 253.
[28] L.F. Errea, L. Mendez, A. Riera, J. Phys. B: At. Mol. Opt. Phys. 15 (1982) 101.